# Numerical determination of the permeability of fibre reinforcement for the RTM process

**Richard Fournier — Thierry Coupez — Michel Vincent**

*Cemef, Ecole des Mines de Paris – UMR CNRS 7635*
*BP 207, F-06904 Sophia Antipolis cedex*
*michel.vincent@ensmp.fr, thierry.coupez@ensmp.fr*

ABSTRACT. *The fibre reinforcement permeability is an important parameter for mould filling in the Resin Transfer Moulding process. It can be experimentally obtained, but the interest of a numerical determination is to test the influence of the fibre arrangement. We build a tool based on the local flow kinematics resolution in an elementary cell containing a representative amount of fibres. A multidomain approach is used. The fibres and fluid domains are described by characteristic functions, and the computation is carried out on the whole domain. This gives a great flexibility for addressing complex reinforcement without meshing difficulty. Examples of results are given for a woven fabric, a mat, and more complex situations, showing the anisotropy induced by the fibres.*

RÉSUMÉ. *La perméabilité des renforts fibreux est un important paramètre dans le procédé d'injection sur renfort (RTM). Elle peut être déterminée expérimentalement, mais l'intérêt d'une simulation numérique est de tester l'influence de l'arrangement des fibres. Nous avons construit un outil basé sur la résolution numérique de l'écoulement local dans une cellule élémentaire contenant une quantité représentative de fibres. Nous avons utilisé une approche multidonaine. Le calcul est mené à l'aide d'un maillage unique dans lequel les domaines occupés par les fibres et le fluide sont décrits par des fonctions caractéristiques. Cette approche permet de traiter les renforts complexes sans difficulté de maillage. On donne des exemples de tissus, de mat, et des situations plus complexes qui montrent l'anisotropie induite par les fibres.*

KEYWORDS: *RTM, permeability, fibrous media, finite element simulation.*

MOTS-CLÉS : *RTM, perméabilité, renfort fibreux, simulation par éléments finis.*

REEF – 14/2005. Composites forming simulation, pages 803 to 818

## 1. Introduction

The Resin Transfer Moulding process involves mould filling with fibre impregnation, heat transfer between the resin, the fibres and the tool, and curing. Each of these steps has an influence on the product quality. A correct filling means that the mould is totally filled and the fibres perfectly impregnated by the polymer, without voids. The flow front evolution, the velocity and pressure fields are also important factors. They are all related to the permeability of the reinforcement, which characterises the resistance of fibres to the flow.

The flow through the fibres is modelled by Darcy's law (Darcy, 1856) which states a linear relationship between the pressure drop and the flow rate. This law can be generalised for anisotropic 3D flows as:

$$\boldsymbol{q} = -\frac{\boldsymbol{K}}{\eta}\nabla P \qquad [1]$$

where $\boldsymbol{K}$ is the permeability tensor, $\eta$ is the resin viscosity, $\boldsymbol{q}$ is the fluid phase average of the velocity vector $\boldsymbol{v}$ defined as:

$$\boldsymbol{q} = -\frac{\boldsymbol{1}}{\Omega}\int_{\Omega_{fluid}} \boldsymbol{v} \qquad [2]$$

$\Omega$ is the volume containing a volume of fluid $\Omega_{fluid}$. $P$ is the intrinsic fluid phase average of the pressure $p$ in the fluid:

$$P = \frac{1}{\Omega_{fluid}}\int_{\Omega_{fluid}} p \qquad [3]$$

The in-plane permeability is experimentally determined by measuring the flow rate and pressure either between parallel plates or in a radial flow (see for instance Adams *et al.*, 1988, Molnar *et al.*, 1989, Chan *et al.*, 1993, Gauvin *et al.*, 1996, Bréard *et al.*, 1998, Daniel *et al.*, 2000, Lundstrom *et al.*, 2000, Amico *et al.*, 2001, Nedanov *et al.*, 2002a). Dispersions in the results are very often reported, because of variation of the fibre structure, and also because of several experimental difficulties, such as the flow racing effect near the mould walls, the mould deflection. This is the reason why we chose to calculate this permeability, which will allow studying the relation between the local arrangement of the fibres on the permeability.

Most permeability models have been based on an approximation of the pore structure. The Carman-Kozeny model (Carman, 1938) has been established for granular media. It provides a simple expression for the permeability as a function of the fibre radius and volume fraction, with a constant function of the pore geometry.

Another technique consists in calculating the velocity – pressure drop relation in a unit cell, assuming incompressible Newtonian flow and then determine the permeability. This has been done for periodic fabrics. Analytical methods can be used for unidirectional fabrics (Gebart, 1992, Hoareau *et al*., 1994, Hoareau, 1994). More realistic arrangements have been considered using fractal geometry description (Pitchumani *et al*., 1999). Numerical methods allow consideration of more or less complex fibre arrangements, such as boundary-integral method (Larson *et al.*, 1986, 1987), finite difference associated to lubrication theory (Simacek *et al.*, 1996), finite element method (Phelan, 1991, Skartsis *et al*., 1992, Gebart, 1992 [10], Hoareau *et al.*, 1994, Hoareau, 1994, Choi *et al.*, 1998, Torres Carot *et al.*, 2001, Takano *et al.*, 2002, Nedanov *et al*., 2002b, Boust *et al.*, 2002). The lattice Boltzmann method (Martys *et al*., 1996, Spaid *et al.*, 1998) solves for the flow in a unit cell, and integrates the fluid velocity distribution to generate a prediction of total flow at a prescribed pressure gradient, which leads to the permeability.

In the previous studies, the tow, which is composed of hundred or thousands of filaments, is considered as fully saturated, and the flow inside it is neglected. The flow inside the tow has been taken into account by Phelan *et al*., (Phelan, 1991, Phelan *et al*., 1993, Phelan *et al.*, 1996), Lekakou and Bader (Lekakou *et al.*, 1998), Simacek and Advani (Simacek *et al.*, 1996, Spaid et *al.*, 1998), Ngo and Tamma (Ngo *et al.*, 2001), Torres Carot *et al.*, 2001. The Stokes equations are used between the tows, and the Brinkman equation (Brinkman, 1947) is used inside the tow (except for Simacek and Advani who used the Darcy's model). This equation is a generalisation of Darcy's law, which includes the Stokes term $\eta\Delta v$ to the expression of the pressure gradient $\nabla P$. It makes possible the matching of velocity and pressure fields at the boundary. The permeability of the tow is needed. This approach is interesting for studying the saturation process, and the air entrapment and void formation. The unsaturated permeability was found to be lower than the corresponding saturated value (Spaid *et al.*, 1998). The influence of the intra-tow permeability on the global permeability increases with the inter-tow packing, that is for quite low permeability values, of the order of $10^{-12}$ $m^2$.

Most of the models are 2D, and consider transverse flow of unidirectional fibres. 3D geometries have been considered by Martys *et al.*, 1996, Ngo *et al.*, 2001, Torres Carot *et al.*, 2001, Takano *et al.*, 2002.

The aim of this work is to propose a finite element model, which allows for the computation of permeability of a large variety of reinforcements, including sheared fabrics, randomly oriented fibre mats, and more complex reinforcements. This flexibility is possible because of a multidomain formulation. The whole cell is meshed, including the tow and inter-tow regions (which are the flow regions).

## 2. Permeability computation

### 2.1. *Principles*

The fibres are supposed to be saturated with fluid, and the flow inside the tows is neglected. The permeability is determined by homogenisation. A unit cell of volume Ω representative of the fibre arrangement is selected. Its size must be large with respect to the fibre size, and small with respect to the scale of the flow to represent local properties. Different cells will be presented in section 3. They are parallelepipedic. The principle is to impose a pressure gradient $\nabla P$ on two opposite sides of the cell, in order to obtain the permeability tensor component $K$ in the direction of the normal of the sides.

The boundary conditions on the other sides of the cell is subject to discussion. For the mats, where fibres are randomly oriented parallel to a plane, we consider a large domain of calculation, and the velocity component normal to the sides (except the two sides where the pressure gradient is imposed) is set to zero. This condition is incorrect, as there is no symmetry in such a reinforcement. This is the reason why the representative volume element (RVE) is a sub-domain, where the influence of the boundary conditions is negligible. The determination of the size of the RVE will be presented in section 3.2.

When the fibres are periodically organised such as in fabrics, we can have two situations. Consider first a square arrangement of unidirectional cylindrical fibres. The RVE can be taken as the unit cell defining the lattice, and a zero normal velocity condition corresponding to symmetry condition is correct. But in more complex fabrics such as those which will be studied in 3.1 or 3.4, the periodicity is not equivalent to symmetry. Therefore, the same technique as for the mat will be used.

A sticking contact is assumed at the fibre tow surface.

$K$ is determined by minimising $|\boldsymbol{v}-\boldsymbol{q}|^2$, where $\boldsymbol{v}$ and $\boldsymbol{q}$ are respectively the local and average velocity:

$$\min_K \int_\Omega 1_{\Omega_f} \left| v + \frac{K}{\eta} \nabla P \right|^2 d\Omega \qquad [4]$$

Writing that the derivative of the integral is equal to 0 leads to:

$$K = -\eta \frac{\int_\Omega 1_{\Omega_f} |v.\nabla P| \, d\Omega}{\int_\Omega 1_{\Omega_f} |\nabla P|^2 \, d\Omega} \qquad [5]$$

Here, Ω must be considered as the RVE, the calculation being carried out on a larger domain.

$\boldsymbol{v}$ is obtained with REM3D®, a finite element software package for 3D mould filling and packing (Pichelin *et al*., 1998). It uses mixed finite elements for flow computation (P1+/P1), discontinuous Galerkin method for both convection and convection diffusion solution (Batkam *et al*., 2004) and a multidomain framework which is entering in the family of VOF method.

The resin is assumed to have an incompressible Newtonian behaviour. Inertia and gravity forces are neglected. The unknowns are the velocity vector $\boldsymbol{v}$ and the pressure $P$. In order to simplify the mesh generation, a unique mesh of the entire cell is considered and the generalised Stokes equation are solved using a penalty technique to enforce a rigid body motion into the fibre domain. For that purpose, a fibre viscosity is introduced (the penalty parameter which optimal value will be studied in section 2.3.3) and a global flow calculation is performed in the entire domain.

The resin and fibres domains are respectively represented by characteristic functions $1_{\Omega fluid}$ and $1_{\Omega fibre}$. The characteristic function values are exactly one or zero. A value of $1_{\Omega fluid}$ of 1 represents the fluid domain and the Stokes equations apply using the normal fluid viscosity. If the value is 0, the domain corresponds to the fibres, and the same equations apply but with a much higher viscosity parameter in order to avoid any deformation of the fibres. However, when the interface between the two domains crosses a mesh element the characteristic function can only be approximated by a fill factor taking all the possible values between 0 and 1 and corresponding to the amount of material intersecting a given element of the mesh. The fill factor calculation is the objective of the next section. The main point of the proposed approach is the fuzzy representation of the interface between the different domains, allowing much more flexibility.

## 2.2. *Characteristic function approximation*

The unit cell, a cube or more generally a parallelepiped, is meshed for the finite element resolution (figure 1a). A second mesh defines the fibres, a cylinder in the simplest case.

The method we developed is equivalent to “print an object on a 3D screen”. The boundary of the screen is the boundary of the cell. The pixels (voxels in 3D) of the screen are placed on a Cartesian grid, with a size much smaller than the finite element size of the cell (Figure 1b). A fibre is introduced in the cell at a given position and orientation (Figure 1c), and “printed” on the screen. This means that the pixels which belong to each finite element of the fibre are set to 1, the other ones remaining at 0 (Figure 1d). Finally, the value of the characteristic function of the fibre in each element of the cell is obtained by counting the number of pixels with value 1 or 0 (Figure 1e). The ratio of the number of pixels of value 1 to the total number of pixels in the element is the value of the characteristic function in the element.

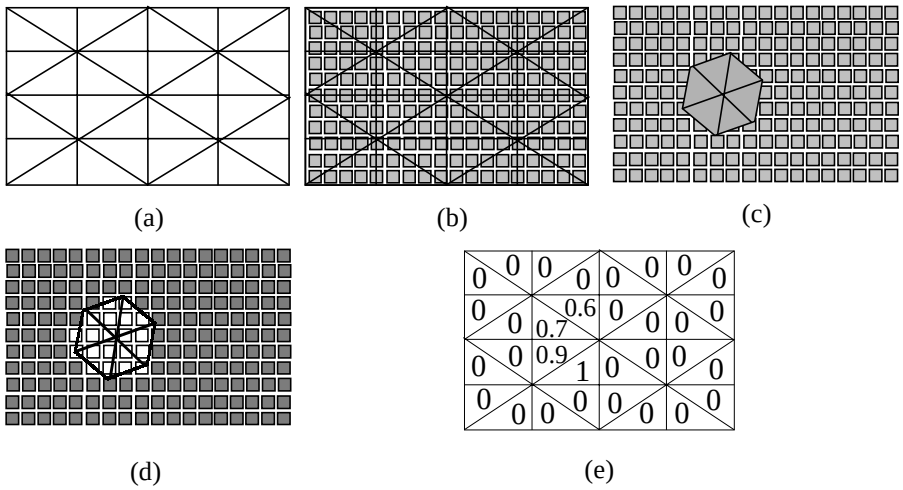


**Figure 1.** *Method for initialisation of the characteristic function of the fibres*

A mesh adaptation technique permits to increase the number of nodes at the fibre surface for the same mesh definition (Bigot, 2002).

### 2.3. *Validation tests*

#### 2.3.1. *Comparison to an analytical solution*

We consider the Poiseuille flow between parallel plaques. The flow rate – pressure relation leads to a permeability $K = h^2/12$, where $h$ is the gap between the plaques. The velocity profile in a Poiseuille flow is parabolic. Our elements are first order in velocity. We build a mesh with about 15 nodes in the thickness which allows a correct capture of the velocity profile. For $h = 1$, we computed a permeability value of 0.0832, close to 1/12=0.0833.

#### 2.3.2. *Validation of the fuzzy interface multidomain approach*

The proposed multidomain approach based on fuzzy representation of the different domains can be compared to the exact meshing method.

The standard method consists in solving the Stokes equations by using a mesh for the flow domain only. Figure 2a represents such a domain with the associated mesh. In the proposed approach, the whole cubic region is meshed, and the flow domain is represented by its characteristic function (Figure 2b). The mesh has been adapted at the interface so that it is precisely defined. It appears on Figure 2b as the thin band with clear grey level. For both methods, the pressure has been imposed at the inlet and exit planes, and a sticking contact is assumed elsewhere.

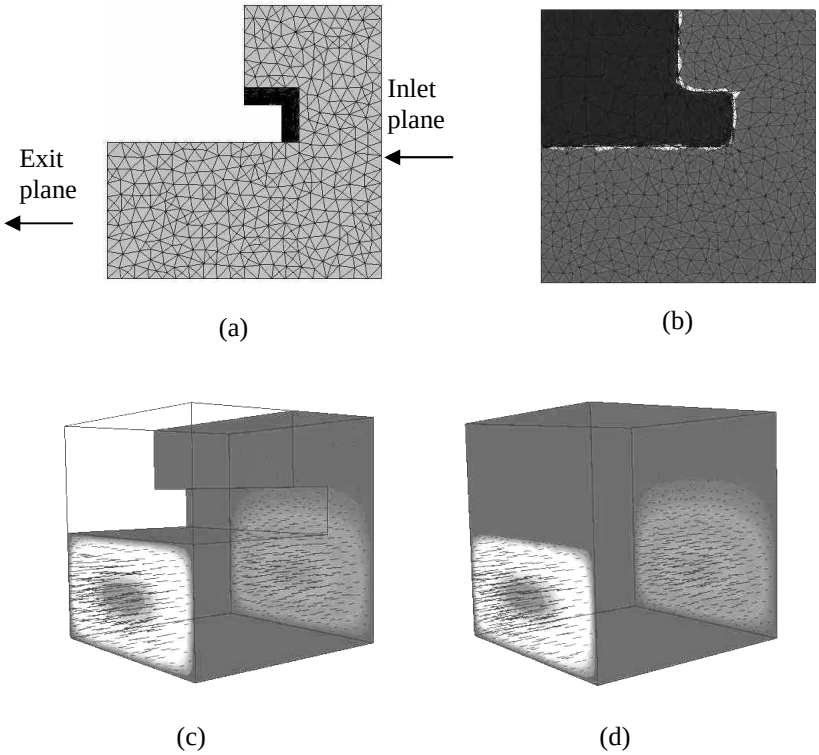


**Figure 2.** *Test domain of the multidomain approach. (a): exact mesh method. (b): multidomain with fuzzy interfaces. It is 1 in the fluid area (intermediate grey), 0 in the solid area (dark grey), and the interface is represented by the clear grey band. (c) and (d): velocity computed with the two methods*

We compared the velocity and pressure fields. For instance, Figure 2c and 2d represent the velocity vectors and values at the entrance and exit planes, for both methods. The values are the same. The same agreement has been found for the pressure field.

2.3.3. *Test of the viscosity of the fibre*

As mentioned in section 2.1, fibres are assumed to be rigid. An easy way to enforce such behaviour is to penalise the strain rate into the fibres. It is equivalent to introduce a fibre viscosity much higher than the fluid one and to continue to solve everywhere the Stokes equations with this local and sudden change in viscosity. The ratio between the fibre and fluid viscosities must be chosen carefully. Numerical experiments showed that it cannot be smaller that $10^2$. If this ratio is included between $10^2$ and $10^5$, the fibre domain remains nearly consistent, but deformations

still occur. If the ratio is larger than $10^5$, fibres behave like a perfect solid, and we chose this value in the following.

## 3. Results

### 3.1. *Woven fabric*

Figure 3 shows the fabric we have studied, and Figure 4 shows the cells with aligned and misaligned stacks. The fibre volume fraction is 44.2%.

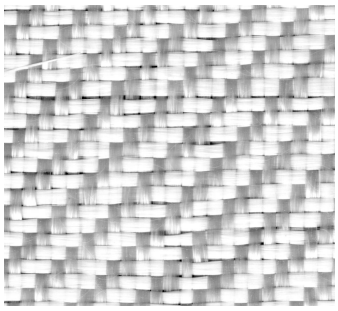

**Figure 3.** *Micrograph of glass fabric*

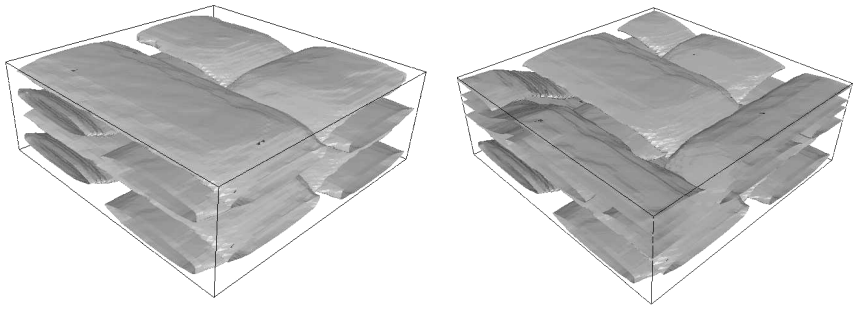

**Figure 4.** *Woven fabric. Aligned stack (left), misaligned (right)*

The in-plane permeabilities in the two directions of the plane are very similar, and no significant difference has been obtained between the two fibre arrangements. Its value is $2.76\ 10^{-9}$ m². The transverse permeability is lower. When the fabric layers are aligned, it is $3.8\ 10^{-10}$ m². When layers are not aligned, the permeability is lower, $3.1\ 10^{-10}$ m².

### 3.2. *Mat*

Figure 5 shows a picture of fibre mat. Fibres are randomly oriented in a plan. For the computation cell, the cylindrical fibres have been randomly generated parallel in a plane. Figure 6 represents a fibre mat cell with a fibre volume fraction of 19%.

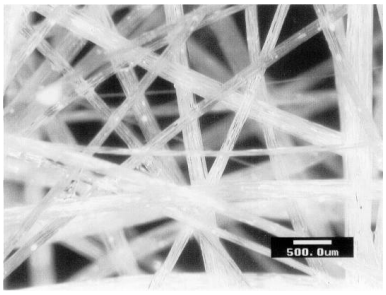


**Figure 5.** *Micrograph of a mat*

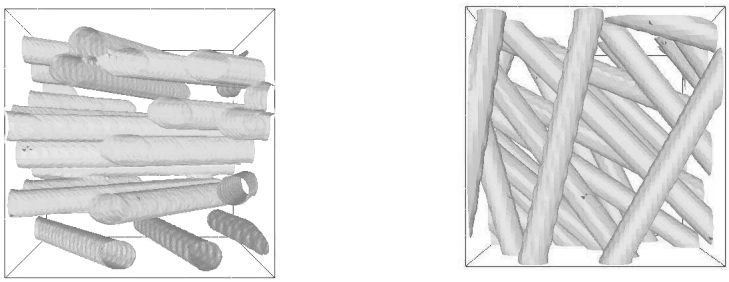

**Figure 6.** *Front view (on the left), top view (on the right) of a fibre mat*

The RVE of the mat must be determined. It must be as large as possible to represent the fibre arrangement. Moreover, as mentioned in section 2.1, the boundary conditions on the sides where the pressure gradient is not imposed must not influence the solution in the volume. For this purpose, we generated a large domain of computation (2.5 mm on Figure 7), and determined the permeability throughout successive sub-volumes. Figure 7 shows that below a size of about 1 mm, the permeability diverges, and above 2 mm, the evolution is weak. We see that when the size of the RVE is equal to the size of the calculation domain (2.5 mm), there is no divergence. This means that the boundary conditions play a minor role. This is due to our method based on a volume minimisation (equations 4 and 5).

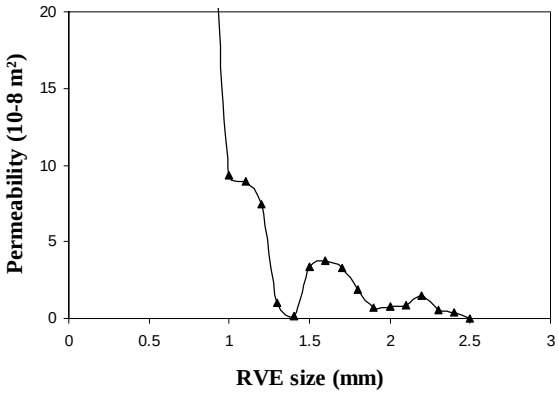


**Figure 7.** *Permeability evolution as a function of the size of the elementary volume*

We are now able to calculate the permeability. The two in-plane permeablities are very similar, 2.1 $10^{-8}$ m², which shows that the isotropy has been respected. The transverse permeability is lower, 6.4 $10^{-9}$ m².

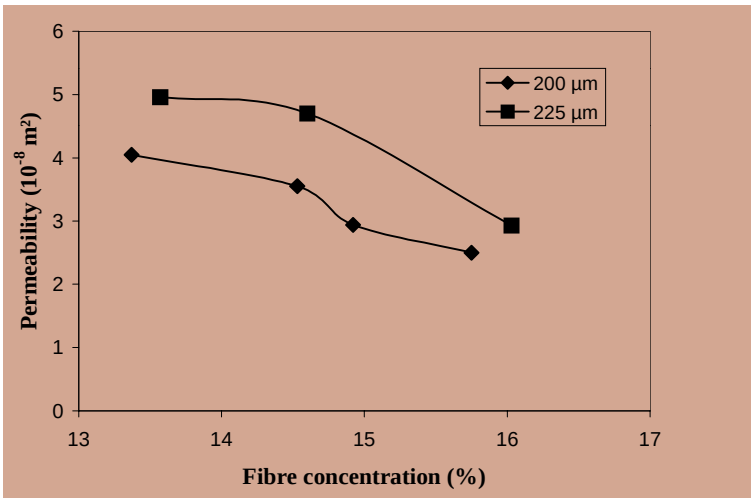


**Figure 8.** *Influence of the tow size on the permeability*

We tested the influence of the size of the fibres. Figure 8 shows that, for a given concentration, when the fibre diameter decreases from 225 to 200 µm, the permeability decreases of about 25 %. This is explained by a topological argument: more fibres are needed to fulfil a given concentration, consequently the distance

between fibres is smaller and the total surface between fibres and liquid (with a null velocity) is larger.

### 3.3. *Rovicore*

The Rovicore® is a sandwich made of a polypropylene core surrounded by two chopped mat layers. According to its producer Chomarat, it is easy to drape, and the resin flow is good. We generated two cells. The first one represents the polypropylene core (Figure 9a). The fibres are randomly distributed in space. The second one represents half of the core, and one layer of fibre mat, with in-plane isotropic orientation (Figure 9b).

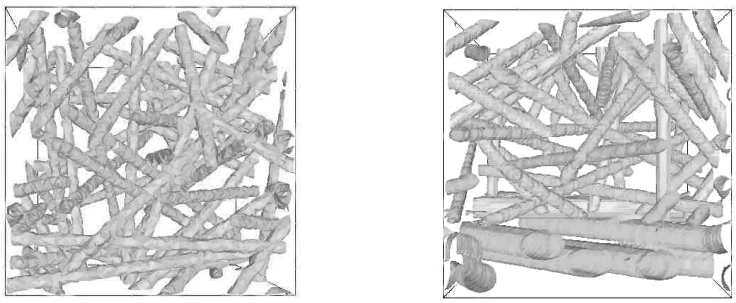

**Figure 9.** *Polypropylene core (left) and polypropylene with one glass mat (right)*

The computed permeability of the core is $2.26\ 10^{-8}$ m² for a fibre volume fraction of 15%, whereas the equivalent in-plane permeability of the whole reinforcement is $1.3\ 10^{-8}$ m². This confirms that the central layer makes the resin flow easier.

### 3.4. *Sheared fabrics*

The objective is to evaluate the influence of a simple shear deformation on the permeability. We considered a simple bi-directional reinforcement, and we applied geometric shearing to the mesh of the reinforcement (Figure 10) which is similar to the picture frame test. The pressure gradient is imposed on the sides normal to the $x$ direction, so the component $K_{xx}$ of the permeability tensor is determined. On the other faces of the cell, we imposed zero normal component of the velocity, equivalent to a slip condition, which is the less perturbing condition for the volume averaged calculation of the permeability (see equations 4 and 5). Moreover, the cell size is larger than the lattice unit cell. The evolution of the permeability is shown on Figure 11. Permeability decreases with the angle of shear.

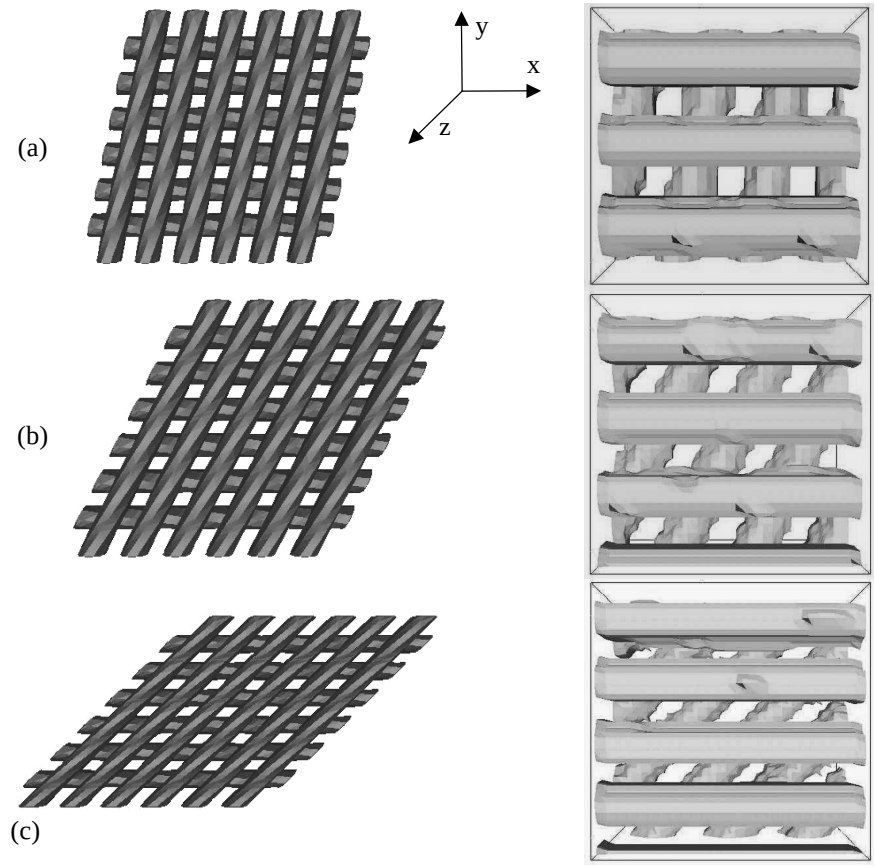


**Figure 10.** *Sheared fabrics at different angles: 11° (a), 26° (b), 45° (c) (on the left), and associated cell (on the right)*

The permeability of the reinforcement sheared at an angle of 45° is determined for different flow directions. This gives the value of the permeability for different reference frames. Instead of changing the flow direction, we rotated the reinforcement in the cell, and the imposed pressure gradient is always in the x direction (Figure 12). Therefore we obtain only one of the 5 components of the permeability tensor (or 3 components in the principal frame), $K_{xx}$, corresponding to fibres making an angle θ with the x direction of the reference frame.

Figure 13 shows that the permeability is minimal for an angle θ around 70°, and maximal for around 160°, which are the principal directions of the permeability tensor.

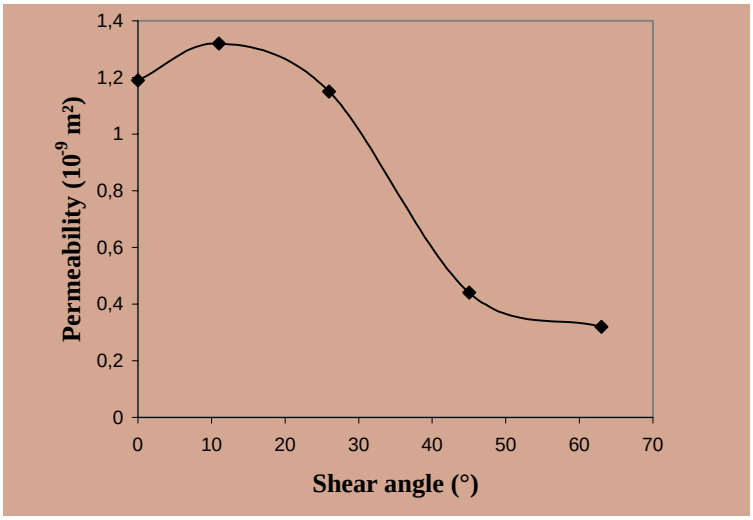


**Figure 11.** *Evolution of the permeability with the angle of shear*

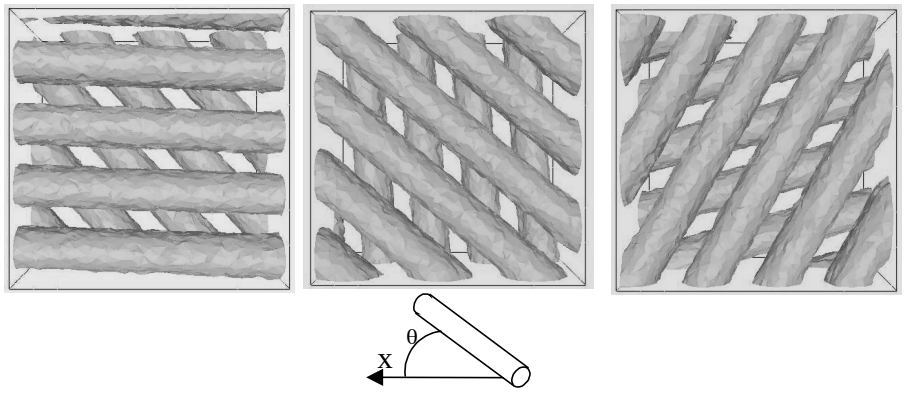


**Figure 12.** *Different orientations of the same sheared reinforcement*

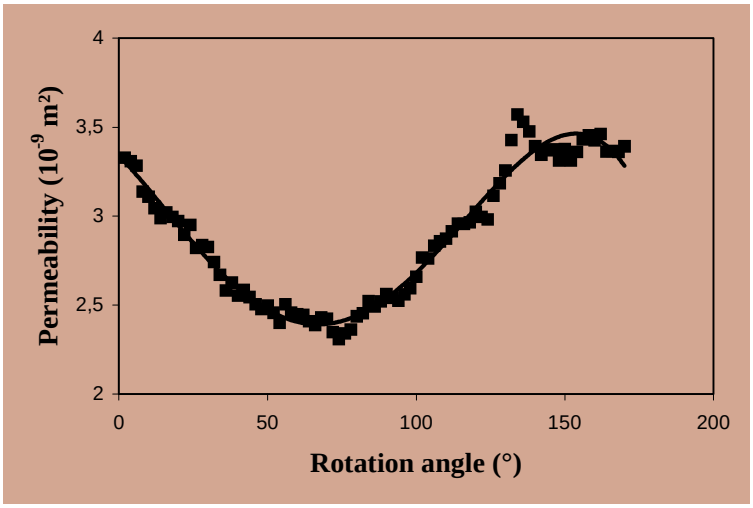


**Figure 13.** *Evolution of the permeability with the angle between the fibre axis and the x direction of the reference frame*

## 4. Conclusions

The permeability of reinforcements for the RTM process has been calculated by using numerical simulation. In order to simplify the meshing operation, multidomain calculations have been performed using a fuzzy interface approach. This very flexible method allows to study of a large variety of reinforcement, including random fibre mats. The anisotropy of permeability has been quantified. Moreover, the simulation can be performed to calculate local values in a mould where the reinforcement has been disturbed by mould closing, and generate more accurate data for a mould filling computation based on Darcy's law.

Acknowledgements

This work has been carried out in the framework of the Predit program funded by the Ministry of transportation. We are grateful of the help provided by the partners involved in this project, and in particular by J.P. Cauchois and G. Cledat from Pôle de Plasturgie de l'Est.

## 5. References

Adams KL, Russel WB, Rebenfeld L., "Radial penetration of a viscous fluid into a planar anisotropic porous medium", *Int J Multiphase Flow*, Vol. 14, No. 2, 1988, pp. 203-15.

Amico S., Lekakou C., "An experimental study of the permeability and capillary pressure in resin transfer moulding", *Compos. Sci. Technol.*, Vol. 61, 2001, pp. 1945-59.

Batkam S, Bruchon. J., Coupez T., "A space time discontinuous Galerkin method for convection and diffusion in injection moulding", *Int. J. Forming Processes*, Vol. 7, No. 1-2, 2004, pp. 11-33.

Bigot E., Simulation tridimensionnelle du remplissage de corps minces par injection, Doctoral Thesis, Ecole Nationale Supérieure des Mines de Paris, France, 2002.

Boust F., Flavin E., Torres-Carrot R., "Modélisation de la perméabilité des renforts fibreux", *Journée scientifique de l'ONERA : Procédé RTM et modélisation*, 2002.

Bréard J., Saouab A., Bouquet G., "Mesure de la perméabilité spatiale d'un renfort tridimensionnel pour les matériaux composites à matrice polymère", *Eur. Phys. J. AP.*, Vol. 1, 1998, pp. 269-278.

Brinkman H.C., "A calculation of the viscous force exerted by a flowing fluid on a dense swarm of particles", *Appl. Sci. Res.*, Vol. A1, 1947, pp. 27-34.

Carman P. C., "Fluid flow through a granular bed", *Trans. Inst. Chem. Eng. London*, Vol. 15, 1938, pp. 120-156.

Chan A. W., Larive D. E., Morgan R. J., "Anisotropic permeability of fiber preforms: Constant flow rate measurement", *J. Compos. Mat.*, Vol. 27, 1993, pp. 996-1008.

Choi M. A., Lee M. H., Chang J., Lee S. J., "Permeability modeling of fibrous media in composite processing", *J. Non-Newt. Fluid Mech*., Vol. 79, 1998, pp. 585-598.

Daniel I. M., Um M. K., Childs B. W., Kim D. H., "Permeability and resin flow measurements and simulations in composite preforms", *45th International SAMPE Symposium*, May 21-25, 2000, pp. 761-775.

Darcy H., *Les fontaines publiques de la ville de Dijon*, Dalmont, Paris (1856).

Gauvin R., Trochu F., Lemenn Y., Diallo L., "Permeability measurement and flow simulation through fiber reinforcement", *Polym. Compos.*, Vol. 17,1996, pp. 34-42.

Gebart B. R., "Permeability of unidirectional reinforcements for RTM", *J. Compos. Mat.*, Vol. 26, 1992, pp. 1100-1133.

Gebart B. R., Analysis of heat transfer and fluid flow in the resin transfer moulding process, Doctoral Thesis, Luleä University of Technology, Sweden, 1992.

Hoareau C., Injection sur renfort: étude du remplissage de moule et détermination théorique de la perméabilité de tissus, Thèse de Doctorat, Ecole des Mines de Paris, 1994.

Hoareau C., Vincent M., "Calculation of fabric permeability and application to mold filling in resin transfer molding", *Comptes rendus des 9$^{e}$ journées nationales sur les composites*, Saint-Etienne, 22-24 novembre 1994, Amac, pp. 25-33.

Larson R.E., Higdon J.J.L., "Microscopic flow near the surface of two-dimensional porous media, Part 1, Axial flow", *J. Fluid Mech.*, Vol. 166, 1986, pp. 449-472.

Larson R.E., Higdon J.J.L., "Microscopic flow near the surface of two-dimensional porous media, Part 2, Transverse flow", *J. Fluid Mech.*, Vol. 178, 1987, pp. 119 - 136.

Lekakou C., Bader M. G., "Mathematical modelling of macro and micro infiltration in resin transfer moulding (RTM)", *Composites Part A*, Vol. 29A, 1998, pp. 29-37.

Lundstrom TS, Stenberg R, Bergstrom R, Partanen H, Birkeland PA., "In-plane permeability measurements: a nordic round-robin study", *Composites A*, Vol. 31, No. 1, 2000, pp. 29-43.

Martys N.S., Chen H., "Simulation of multicomponent fluids in complex three-dimensional geometries by the lattice Boltzmann method", *Physical Review E*, Vol. 53, No. 1, 1996, pp. 743-750.

Molnar J.A., Trevino L., Lee L.J., "Liquid flow in molds with prelocated fiber mats", *Polym Compos*, Vol. 10, No. 6, 1989, pp. 414-23.

Nedanov P. B., Advani S. G., "A Method to Determine 3D Permeability of Fibrous Reinforcements", *Journal of Composite Materials*, Vol. 36, No. 2, 2002a, pp. 241-254.

Nedanov P. B., Advani S. G., "Numerical computation of the fiber preform permeability tensor by the homogenization method", *Polymer Composites*, Vol. 23, 2002b, pp. 758-770.

Ngo N.D., Tamma K.K., "Microscale permeability predictions of porous fibrous media", *Int. J. Heat Mass Transfer*, Vol. 44, 2001, pp. 3135-3145.

Phelan F.R., "Modeling of microscale flow in fibrous porous media", *in Advanced composite materials: new developments and applications, proceedings of the 7th annual ASM/ESD advanced composites conference, ASM International*, Detroit, Sept. 30-Oct. 3, 1991, pp. 175-185.

Phelan F.R., Leung Y., Parnas R., "Modeling of microscale flow in unidirectional fibrous porous media", *J. Thermoplastic Compos. Mater*., Vol. 7, 1994, pp. 208-218.

Phelan Jr F. R., Wise G., "Analysis of transverse flow in aligned fibrous porous media", *Composites Part A*, Vol. 27A, 1996, pp. 25-34.

Pichelin E., Coupez T., "Finite element solution of the 3d mold filling problem for viscous incompressible fluid", *Comput. Methods Appl. Mech. Engrg*., Vol. 163, 1998, pp. 359-371.

Pitchumani R., Ramakrishnan B., "A fractal geometry model for evaluating permeabilities of porous preforms used in liquid composite molding", *Int. J Heat Mass Transfer*, Vol. 42, 1999, pp. 2219-2232.

Simacek P., Advani S.G., "Permeability model for a woven fabric", *Polym. Compos.*, Vol. 17, No. 6, 1996, pp. 887-899.

Skartsis L., Khomani B., Kardos J.L., "Resin flow through fiber bed during composite manufacturing processes, Part II: numerical and experimental studies of Newtonian flow through ideal and actual fiber beds, *Polym. Eng. Sci.*, Vol. 32, No. 4, 1992, pp. 231-239.

Spaid M.A.A., Phelan F.R., "Modeling void formation in fibrous porous media with lattice Boltzmann method", *Composites Part A*, Vol. 29A, 1998, pp. 749-755.

Takano N., Zako M., Okazaki T., Terada K., "Microstructure-based evaluation of the influence of woven architecture on permeability by asymptotic homogenization theory", *Compos. Sci. Tech.*, Vol. 62, 2002, pp. 1347-1356.

Torres Carot R., Boust F., Poitou A., "The concept of permeability in the Resin Transfer moulding process: Darcy's law and multiple porosity", *Proceedings of ESAFORM 2001*, Liège (Belgium), April 23-25, 2001, pp. 167-170.